ACS APPLIED MATERIALS & INTERFACES

Research Article

www.acsami.org

Soft-Matter Printed Circuit Board with UV Laser Micropatterning

Tong Lu,[†] Eric J. Markvicka,[‡] Yichu Jin,[†] and Carmel Majidi*[,†,‡]

[†]Department of Mechanical Engineering and [‡]Robotics Institute, Carnegie Mellon University, Pittsburgh, Pennsylvania 15213, United States

Supporting Information

ABSTRACT: When encapsulated in elastomer, micropatterned traces of Ga-based liquid metal (LM) can function as elastically deformable circuit wiring that provides mechanically robust electrical connectivity between solid-state elements (e.g., transistors, processors, and sensor nodes). However, LM-microelectronics integration is currently limited by challenges in rapid fabrication of LM circuits and the creation of vias between circuit terminals and the I/O pins of packaged electronics. In this study, we address both with a unique layup for soft-matter electronics in which traces of liquid-phase Ga−In eutectic (EGaIn) are patterned with UV laser micromachining (UVLM). The terminals of the elastomer-sealed LM circuit connect to the surface mounted chips through vertically aligned columns of EGaIn-coated Ag−Fe_2O_3 microparticles that are embedded within an interfacial elastomer layer. The processing technique is compatible with conventional UVLM printed circuit board (PCB) prototyping and exploits the photophysical ablation of EGaIn on an elastomer substrate. Potential applications to wearable computing and biosensing are demonstrated with functional implementations in which soft-matter PCBs are populated with surface-mounted microelectronics.

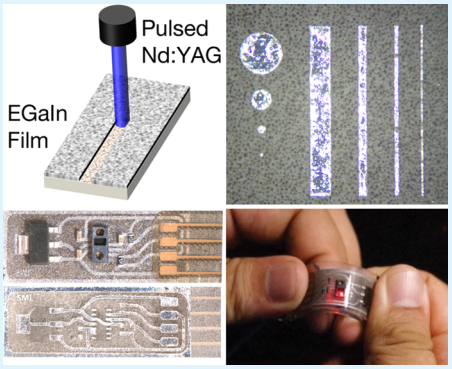

KEYWORDS: *eutectic gallium−indium, liquid metal, conductive elastomers, anisotropic conductivity, stretchable electronics, wearable computing, biomonitoring, photonic biosensing*

1. INTRODUCTION

Skin-mounted electronics for wearable computing and health monitoring require stretchable circuits that match the mechanical properties of soft natural tissue.[1] Current approaches include so-called "deterministic architectures" in which mechanical compliance is introduced through geometry (e.g., PANI or Ag−Ni alloy coated on a woven fabric[2−5] or thin metal interconnects with serpentine[6,7] or prebuckled wavy[8−10] geometries). Because the conductive materials are intrinsically rigid (elastic modulus ≥ 1 GPa) and inextensible, stretchable functionality must be engineered through microscale geometric design and cleanroom fabrication. Another popular approach is to use conductive polymers and composites that are intrinsically soft and deformable. Polyurethanes (PU), polydimethylsiloxane (PDMS), polyacrylates, fluoropolymers, and styrene ethylene butylene styrene copolymer (SEBS) are typically used as the carrier medium. In order to be conductive, they are typically embedded with percolating networks of rigid metallic nano-/microparticles[11,12] or carbon allotropes (e.g., MWCNT, graphene)[13−17] or grafted with polyaniline, ionomers (e.g., PEDOT:PSS), and other conductive polymer groups.[18,19] While promising for low-load/moderate-strain applications, these composites are typically more rigid and less elastic than homogeneous elastomers, stretchable elastene fabrics, or natural biological tissue. Nonetheless, they have adequate mechanical properties for electronic skin applications and can be patterned using a variety of rapid fabrication methods.[20−22]

Liquid metal (LM)-based circuits represent a versatile alternative for stretchable electronics that bypass some of the limitations of deterministic architectures and polymer composites.[23,24] Ga-based LM alloys like Ga−In eutectic (EGaIn; 75% Ga and 25% In, by weight) and Ga−In−Sn (Galinstan; 68% Ga, 22% In, 10% Sn) are particularly attractive because of their low viscosity (2 mPa·s), high electrical conductivity (3.4×10^6 S/m), low melting point (−19 °C for Galinstan), low toxicity, and negligible vapor pressure.[25,26] When encapsulated in a soft elastomer (e.g., PDMS), liquid-phase traces of Ga-based alloy can provide highly robust electrical connectivity between solid-state elements within a circuit and enable extreme elastic deformability. Another feature of Ga-based LM alloys is that in O_2-rich environments like air they form a self-passivating surface layer of Ga_2O_3 (thickness ∼1−3 nm) that dramatically reduces surface tension and allows patterned traces to hold their shape.[27−29]

This oxidation and moldability has enabled EGaIn to be patterned with a variety of techniques[26,30] based on stencil lithography,[31,32] selective wetting,[33,34] reductive patterning,[35] microcontact printing,[28,36−38] jetting,[39] and 3D direct-write printing.[40−42] Since the mid 2000s, EGaIn microfluidic systems have been engineered for a broad range of applications.[23,24] In the last couple of years, this includes continued efforts in

Received: April 20, 2017
Accepted: June 12, 2017
Published: June 12, 2017

DOI: 10.1021/acsami.7b05522
ACS Appl. Mater. Interfaces 2017, 9, 22055−22062

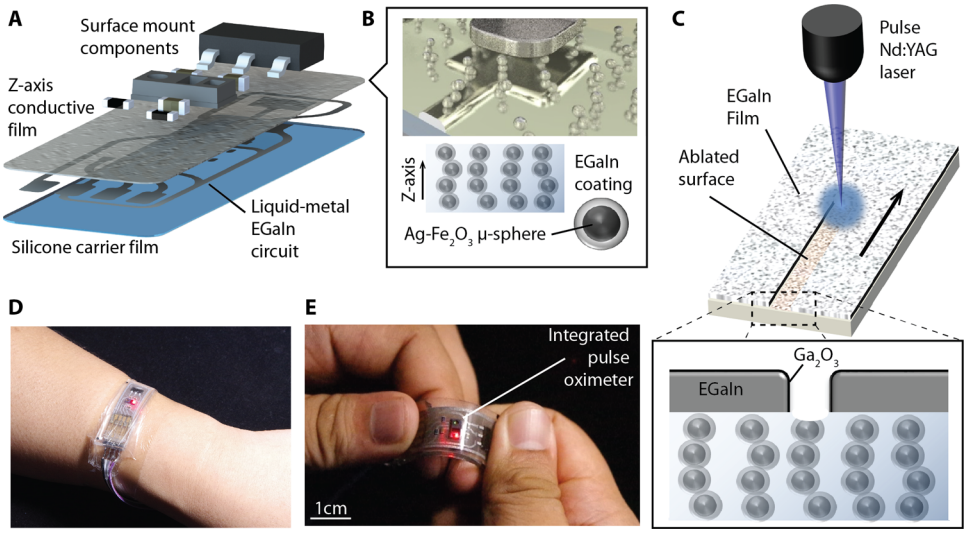

Figure 1. Liquid–metal soft-matter electronics. (A) Illustration of soft-matter bioelectronic skin. (B) Vertically aligned columns of Ag–Fe_2O_3 microparticles coated in EGaIn act as *z*-axis interconnects between LM trace terminals and surface-mounted components. (C) Illustration of EGaIn patterned using UVLM. During patterning within an oxygen-rich environment, the growth of Ga_2O_3 is necessary to hold the shape of the LM circuit (see inset). (D) Soft-matter bioelectronic skin with integrated pulse oximeter that can be worn as a wrist band and (E) support mechanical deformation during operation.

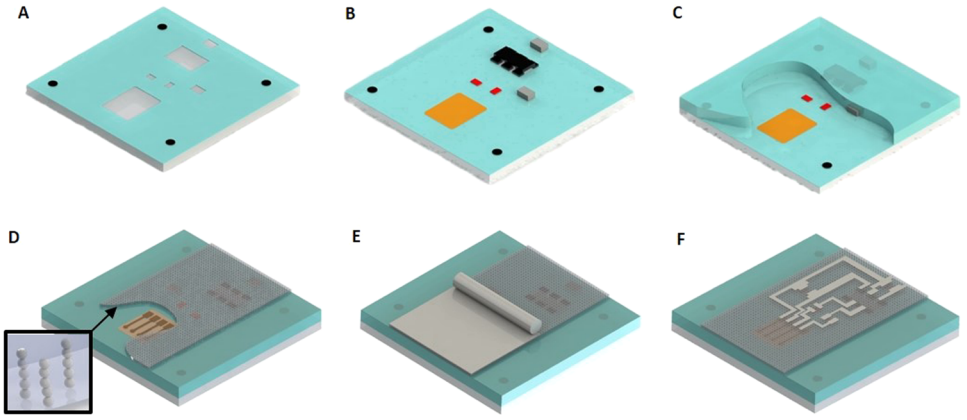

Figure 2. Fabrication process with UVLM. (A) PDMS substrate is applied onto a glass plate. Placement openings and fiducials are patterned with UV laser for placing surface mount components and laser alignment, respectively. (B) Surface mount electronic components are placed into the openings with PVA as a bonding agent. (C) The components are then sealed in PDMS. (D) The chip-embedded elastomer is peeled from the glass plate, flipped over, and coated with a layer of zPDMS. (E) A film of EGaIn is applied on the zPDMS with a PDMS roller and then (F) patterned with a UVLM system. Lastly, the LM circuit is sealed in PDMS and released from the glass substrate.

sensing and electromechanical transducers,[43−50] force characterization for medical endoscopy,[51] reconfigurable metamaterials,[52,53] and radio antennae that exhibit tunable operating frequency and enhanced range.[54−61]

Despite their extraordinary potential, progress in LM electronics is currently limited by methods for integration with MOSFETs, microprocessors, chipsets, cable adapters, and other solid-state technologies (SSTs). Recent efforts with so-called dual-trans printing[38] and *z*-axis conductive elastomer[62] have successfully addressed integration but only with millimeter-scale pins and traces. Successful integration of LM-based circuits and microscale SSTs requires processing techniques that are (i) compatible with conventional PCB manufacturing, (ii) enable reliable interfacing between the terminals of the LM circuit and I/O pins of packaged electronics, and (iii) allow for planar circuit features with dimensions below 100 μm.

Here, we report a unique layup for LM-based soft-matter electronics that simultaneously addresses these challenges through innovations in materials selection and processing (Figure 1A). As in conventional PCB prototyping, a UV laser micromachining (UVLM) system (Protolaser U3; LPKF) is used to pattern an ∼20 μm coating of LM on a polymer substrate. The Protolaser U3 is a Nd:YAG laser with 355 nm wavelength, 200 kHz pulse rate, and 15 μm diameter beam that is capable of direct photophysical ablation of metal. Using a 1 W beam power, the liquid metal features can be reliably patterned with planar dimensions of 50 μm. In contrast, previous attempts at EGaIn patterning with a CO_2 laser require indirect material expulsion through vapor recoil force that limits the minimum feature size to ∼250 μm.[63] We also show that UVLM-patterned EGaIn circuits can interface with surface-mounted SSTs using an anisotropically conductive "*z*-axis film" composed of vertically aligned columns of EGaIn-coated Ag–Fe_2O_3 μ-spheres embedded in a PDMS matrix (Figure 1B).

DOI: 10.1021/acsami.7b05522
ACS Appl. Mater. Interfaces 2017, 9, 22055−22062

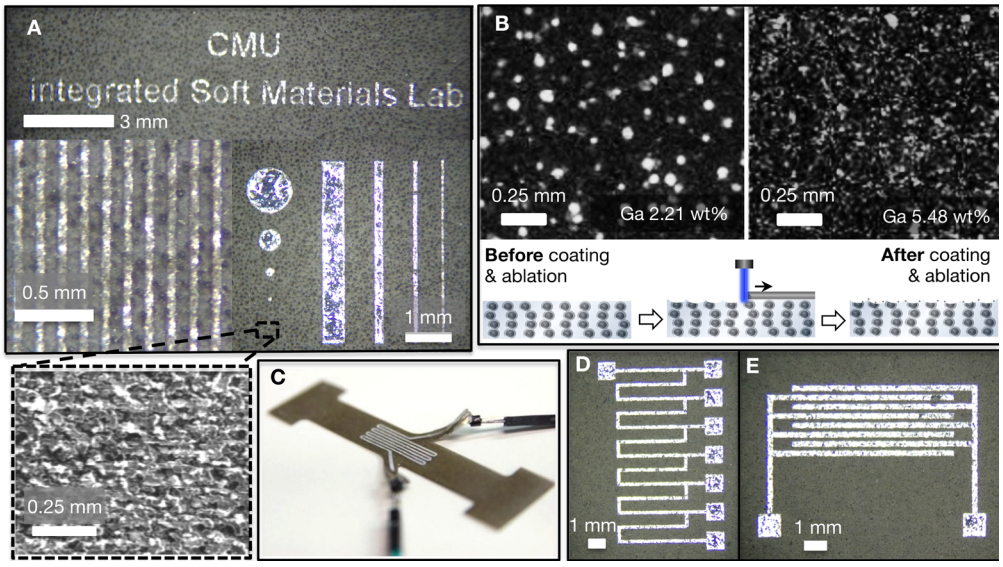

Figure 3. Samples of UV laser-patterned EGaIn features. (A) The planar dimensions of patterned traces can be as small as 50 μm. The SEM image in the inset shows the rough surface of zPDMS after laser ablation. (B) The EDS image of elemental distribution of Ga before and after EGaIn coating and laser ablation. (C) Serpentine circuit used to measure electrical resistance during stretch. (D) EGaIn circuit with multiple terminals for measuring the influence of trace length on resistance. (E) Interdigitated capacitor for measuring trace length on capacitance.

Unlike conventional *z*-axis films with "dry" ferromagnetic microparticles,[62] the LM-coating allows for electrical connectivity even as the rigid μ-spheres separate under mechanical deformations induced by circuit bending, stretching, or twisting.

As with EGaIn stencil lithography and additive manufacturing, the ability to laser-pattern EGaIn on an elastomeric substrate depends on the formation of a self-passivating, nanometer-thin Ga_2O_3 "skin." The oxide skin allows the patterned liquid metal to hold its shape after laser ablation (Figure 1C) and during deposition of an elastomer seal. This feature of liquid moldability is critical for extending conventional UVLM PCB prototyping to Ga-based LM alloys. Combining UVLM processing with liquid metal and *z*-axis connectivity allows for a versatile method to produce elastically deformable electronics that are mechanically robust and compatible with natural human tissue. Referring to Figure 1D,E, potential applications include an elastomeric band that contains a surface-mounted pulse oximetry unit for reflective photoplethysmogram (PPG) recordings. The PPG waveforms can be used to noninvasively measure blood oxygenation saturation and heart rate, which in turn can be used for tracking physical activity and monitoring a broad range of health conditions.[64] As with other recent photonic bioelectronic devices,[65,66] the circuit is naturally soft and flexible and can conform to the skin without requiring significant attachment forces.

2. RESULTS

Soft-matter PCBs with embedded LM wiring are produced using the fabrication steps presented in Figure 2, details of which are presented in Section S1 of the Supporting Information. The steps presented in Figure 2A–C involve embedding SST chips inside a layer of PDMS (Sylgard 184; 10:1 base-to-curing agent ratio; Dow Corning) such that the board side of the chips are exposed and flush with the elastomer surface. As shown in Figure 2D, the exposed chips are covered with an uncured layer of zPDMS that is composed of the following: 35 wt % 40 μm diameter Ag-coated Fe_2O_3 particles (20% Ag by weight; SM40P20, Potters Industries, LLC), 15 wt % EGaIn (75 wt % Ga and 25 wt % In; Gallium Source), and 50 wt % PDMS. Before adding PDMS, the Ag–Fe_2O_3 and EGaIn are mixed together so that the ferromagnetic microspheres have an LM coating, as illustrated in Figure 1B. Next, the zPDMS layer is deposited on top of the exposed SSTs with a spin coater (1500 rpm for 10s; KW-4A, SPI) and is then cured in an oven (100 °C for 20 min) while the entire sample is placed on top of a flat magnet (~1448 G, 2 in. × 2 in. × 1/4 in. NdFeB; K&J Magnetics, Inc.). As the elastomer cures, the applied magnetic field causes the EGaIn-coated ferromagnetic particles to assemble into vertically aligned columns. After the zPDMS layer is cured, it is coated with a ~20 μm thick film of EGaIn that is then patterned using UVLM. Laser ablation is performed with a beam power of 1 W and marking speed of 150 mm/s.

As shown in Figure 3A, a film of EGaIn on zPDMS can be patterned into features with dimensions as small as 50 μm. The widths of the traces are 500, 200, 100, and 50 μm and the diameters of the circles are 1000, 500, 200, and 100 μm, respectively. For the selected laser settings (1 W power, 150 mm/s mark speed), the trace width and spacing are limited to 50 and 100 μm, respectively, which is consistent with conventional PCB manufacturing. If it is narrower than 50 μm, then there is a significant likelihood that the traces can be nonconductive due to poor localized wetting or excessive removal of EGaIn. Likewise, for minimum line spacings below 100 μm, residue from unablated EGaIn or the presence of EGaIn-coated ferromagnetic particles could lead to in-plane electrical shorting.

As shown by the scanning electron microscopy (SEM) (FEI Quanta 600) image presented in the inset of Figure 3A, the laser not only removes EGaIn but will also texture the zPDMS substrate. The effect of laser ablation on EGaIn removal is further examined by comparing Ga content on the surface of a zPDMS substrate before and after coating and ablation (Figure 3B) using energy dispersive spectroscopy (EDS). For uncoated and unablated zPDMS, Ga is mostly observed on the surface of

DOI: 10.1021/acsami.7b05522
ACS Appl. Mater. Interfaces 2017, 9, 22055–22062

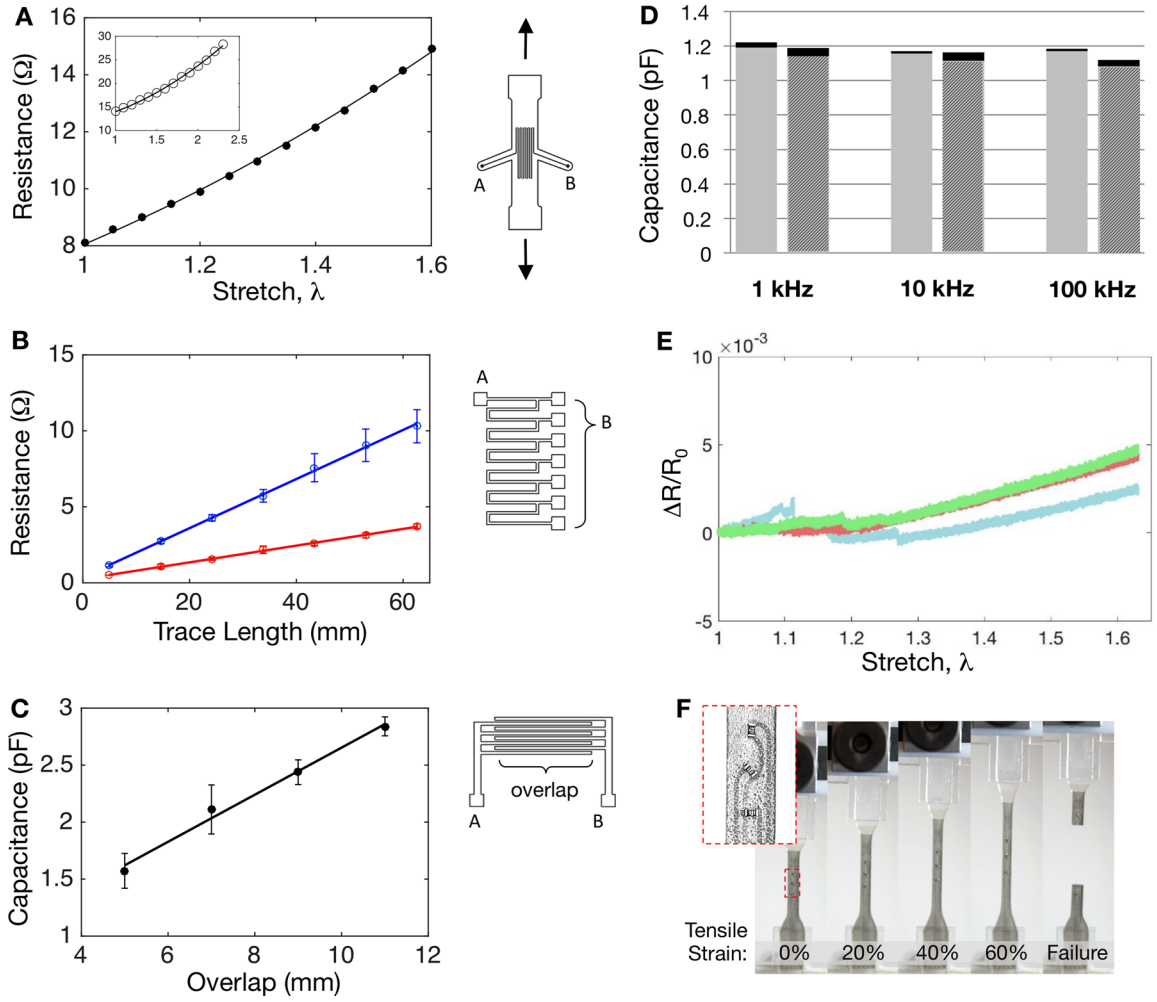

Figure 4. UVLM patterned planar resistors and capacitors. (A) Experimental measurements (markers) and theoretical fit (curve) for electrical resistance versus stretch for serpentine LM trace (120 mm length, 0.5 mm width); Inset: measurement of laser-patterned LM trace encapsulated between two layers of soft polyacrylate elastomer (VHB Tape 4910; 3M). (B) Resistance versus trace length for 100 μm (red) and 200 μm wide (blue) traces. Markers and curves correspond to experimental measurements and theoretical fit, respectively. (C) Experimental measurements (markers) and theoretical fit (curve) for capacitance versus overlap length of interdigitated LM traces (250 μm width, 150 μm spacing). (D) Average capacitance of comb capacitors patterned with (gray) UVLM and (hatched gray) stencil lithography for various testing frequencies. The black bars are the standard deviation (N = 9). (E) Plot of change in electrical resistance versus stretch for surface mount resistors oriented at 0° (blue), 45° (red), and 90° (green). (F) Photographs of sample when strained (0, 20, 40, and 60%) and after failure. Inset: Close up of sample showing placement of resistors. All circuits were pattern on zPDMS unless otherwise noted.

the ferromagnetic particles that support z-axis conductivity in the zPDMS. After an EGaIn coating is applied and removed by UVLM, the substrate is found to be covered in a uniform coating of Ga residue. Moreover, coating and ablation results in an increase in Ga weight fraction (from 2.21 to 5.48 wt %) as shown in Figure 3B, which suggests that not all of the EGaIn coating is ablated. Similar results are observed with EDS analysis of In content (weight fraction increases from 0.51 to 1.27 wt %), as shown in Figure S1. The laser fume extraction system evacuates any of the ablated particles that become airborne (CSA626, Quartro Air Technologies Inc.). In conventional UVLM-based PCB fabrication, this same exhaust system is used to remove 120 μm × 20 mm strips of copper from a copper clad substrate.

The electrical and electromechanical properties of UV laser-patterned EGaIn traces on zPDMS are examined using a variety of circuit designs (Figures 3C–E and 4A–C). A serpentine EGaIn trace is used to measure electrical resistance as a function of stretch (Figure 4A). The serpentine part of the EGaIn trace is 120 mm long and 0.5 mm wide and stretched to 60% strain (in increments of 5%). Resistance versus stretch is fitted using the following Ohm's Law formulation: $R = R_0 + R_1\lambda^2$, where R_0 = 3.7 Ω is the resistance of the leads and R_1 = 4.3 Ω is the initial resistance of the unstretched serpentine trace. Stretch, λ, is defined as the final length of the sample divided by its initial length. Beyond 60% strain, the sample fails mechanically (as further discussed below). In contrast, UVLM-patterned LM traces encapsulated between two layers of soft polyacrylate elastomer (VHB Tape 4910; 3M) can be stretched beyond 125% strain (Figure 4A, inset). Ohm's law is also used to predict the linear influence of trace length on electrical resistance for EGaIn traces of widths 100 and 200 μm (Figure 4B; $R^2 > 0.96$).

Capacitance is measured with interdigitated electrodes of 250 μm width, 150 μm spacing, and varying overlap length (Figure 4C). As expected from electrostatic field theory (see Supporting Information Section S2 and Figure S4), the dependence of capacitance on overlap length is approximately

DOI: 10.1021/acsami.7b05522
ACS Appl. Mater. Interfaces 2017, 9, 22055–22062

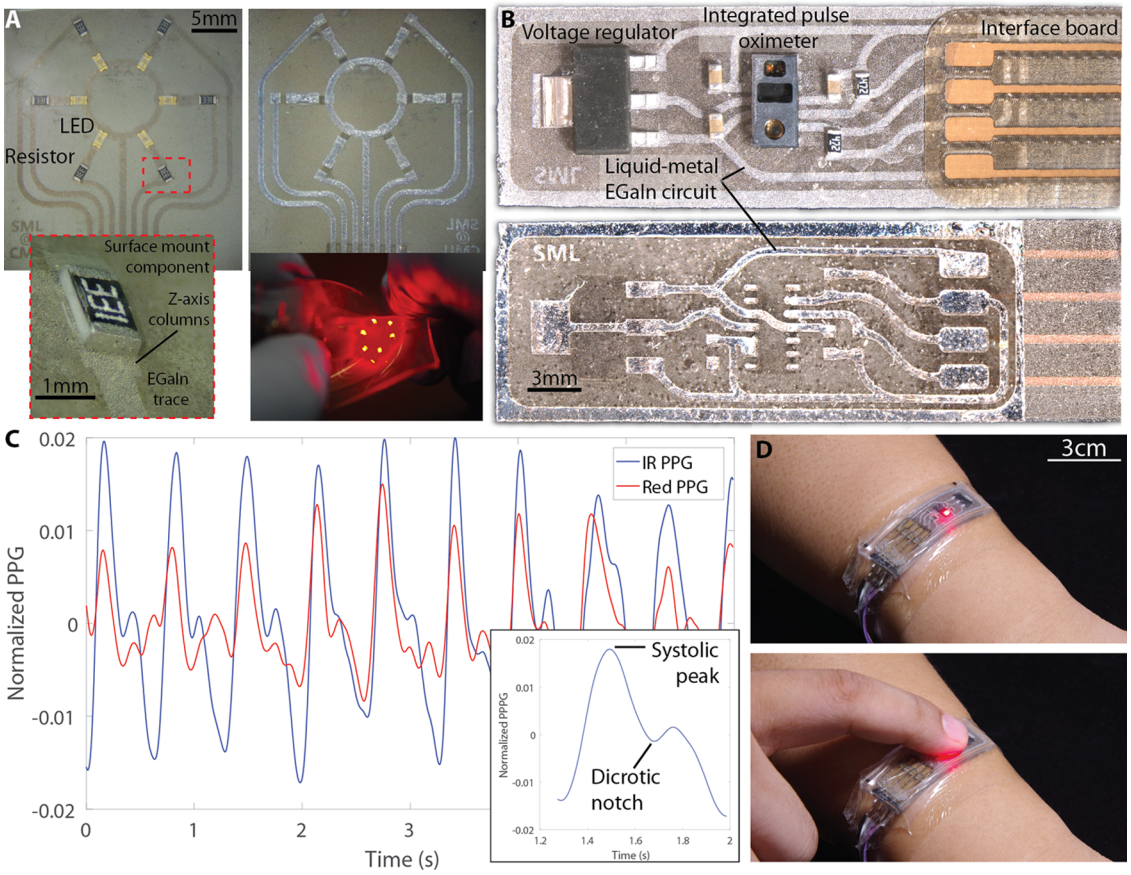

Figure 5. Soft-matter printed circuit board implementation. (A) Top and bottom of a circuit containing a circular array of LEDs. Inset, bottom left: close up of interface between resistor and EGaIn trace; inset, bottom right: soft-matter LED array undergoing deformation during operation. (B) Top and bottom of soft-matter pulse oximeter circuit. (C) PPG waveform recorded from soft-matter pulse oximeter shown in (B); (C) inset: magnified view of single cardiac beat from the measured PPG waveform. (D) Possible implementation of soft-matter pulse oximeter worn as wristband. PPG waveform can be recorded by placing finger on top of wristband while applying light pressure.

linear ($R^2 > 0.9$). The laser-processed method was compared to stencil lithography and is statistically similar (Figure 4D). Lastly, a soft-matter printed circuit board with three 331 Ω surface mount resistors oriented at 0, 45, and 90° was characterized under tensile loading to evaluate performance. The sample was loaded at 10 mm/min, and only a modest increase in resistance (<10%) was recorded until mechanical failure occurred at slightly over 60% strain (Figure 4E,F). This suggests that tensile loading had only negligible influence on the contact resistance between the chip pins, zPDMS, and LM leads.

3. DISCUSSION

With the method presented in Figure 2, packaged SST chips can be embedded in elastomer and wired together with EGaIn interconnects that share dimensions similar to those of conventional copper PCB traces (≥50 μm (2 mil) width, ≥100 μm (4 mil) spacing). The experimental results reported above show that the UV laser-patterned EGaIn traces exhibit properties consistent with classical predictions for electrical resistance and capacitance. However, as noted, the patterning resolution of EGaIn with UVLM is limited by excess liquid metal that remains on the surface after laser processing. This condition is confirmed by comparing SEM and EDS scans of bare zPDMS and those of surfaces that have been coated with EGaIn and then ablated. In particular, we observe a scattering of droplets with dimensions ∼1−10 μm that are rich in Ga and In (Figure S2). Although diffusely scattered, the likelihood that these droplets induce in-plane shorting becomes significant when the spacing between circuit features is below 100 μm.

On the basis of the electrical resistance measurements presented in Figure 4A,B and the known resistivity of EGaIn, we can use Ohm's law to infer trace thickness. For a volumetric resistivity of 29.4×10^{-8} Ω·m,[25] we measure nominal thicknesses ranging from 16.3 to 27.1 μm with no correlation to trace width or pattern geometry. This is roughly consistent with the 17.8 μm average thickness measured for an EGaIn-coated sample that was frozen with liquid nitrogen and then shattered to expose its cross-section for image analysis (Figure S3A). The variation in film thickness is attributed to the nonuniform thickness of the EGaIn film prior to UVLM patterning. While not a critical factor for circuit functionality, the deposition method could be improved to ensure a more uniform distribution and tighter control on EGaIn film thickness. One possible solution is to adopt the atomized spraying technique introduced by Jeong et al. in which LM alloy is deposited using an airbrush and pressure regulator.[32] It should also be noted that visual examination of the sample cross sections suggest that Ag−Fe_2O_3 particles are coated with EGaIn and that liquid bridging between particles can be observed (Figure S3B).

From the slope of the fitted curve in Figure 4C, the effective relative permittivity of the zPDMS substrate can be approximated as $\epsilon_r \approx 5.6$. This calculation is based on a

DOI: 10.1021/acsami.7b05522
ACS Appl. Mater. Interfaces 2017, 9, 22055−22062

theoretical prediction for the capacitance of interdigitated electrodes introduced by Gevorgian et al.[67] (see Supporting Information Section S2). This relatively large permittivity is likely a result of the EGaIn-coated ferromagnetic μ-spheres, which induce an "artificial dielectric" effect[68] within the elastomeric matrix.

As shown in Figure 4D, capacitance measured with electrodes deposited using stencil lithography (1.13 ± 0.05 pF; N = 9) is statistically similar to that for the laser-processed electrodes (1.19 ± 0.03 pF; N = 9). The small discrepancy could be related to additional contributions to the artificial dielectric effect from EGaIn residue that remains after laser ablation. Regardless, such a dielectric enhancement will not influence circuit functionality since the composite remains as an electrical insulator within the plane. This is confirmed by the low dielectric loss tangent, which remains well below 0.1 for the 1 and 10 kHz measurements. It should also be noted that unlike in typical circuits, the substrate on which the metal is patterned is electrically anisotropic, with enhanced permittivity in the plane and conductivity through the thickness.

As shown in Figure 4E, the soft-matter PCB is capable of being stretched with a tensile strain of greater than 60%. The device fails at 62.7% strain due to mechanical failure within the center of the sample. During tensile loading, the encapsulating PDMS layer delaminates from the surface mount component, causing mechnical failure at 62.7% strain (Figure S5). During the experiment, all three resistors experience less than 0.6% change in resistance. It is significant that the strain limit is governed by mechanical rather than electrical failure. This suggests that a higher strain limit may be possible by selecting a more elastic substrate, such as VHB tape (see Figure 4A inset).

The layup and fabrication process presented in Figure 2 is used to produce several representative circuits that integrate UVLM-patterned traces of EGaIn with packaged SSTs (Figure 5). This includes an array of surface-mounted LED and 331 Ω resistor chips (Figure 5A; Figure). We have also fabricated a soft-matter bioelectronic circuit for noninvasive measurements of heart rate (HR) and arterial blood oxygenation (SpO_2). Shown in Figure 4B, the circuit contains an integrated pulse oximetry unit (MAX30100; Maxim Integrated Products, Inc.) that houses a red and IR LED, photodetector and optics, and a low-noise analog signal processor for reflective PPG waveforms (details in Supporting Information Section S3 and Figure S6). A flex PCB with Cu traces is used as an interface board that connects the circuit to a battery-powered Bluetooth module that transmit signals to a host computer for signal processing.[69] The device is configured to collect the PPG waveforms at 200 Hz using LED pulse widths of 400 μs and a current of 20.8 mA (Figure 5C). With appropriate filtering and calibration, the waveforms can be used to obtain HR from spacing of Systolic peaks and SpO_2 by comparing the amplitude (i.e., optical reflection) of IR and red light, which are absorbed differently by oxygenated or deoxygenated hemoglobin within arterial blood.[70] Because the circuit board is intrinsically soft and deformable, the pulse oximetry band can wrap around the wrist and form intimate contact with skin with limited interfacial pressure (Figure 5D).

4. CONCLUSION

We report on a novel layup and processing technique to produce soft and deformable circuits with liquid metal and UV laser micromachining. In order to match the mechanical properties of soft natural tissue, the relatively stiff materials typically used in existing PCBs (metal wiring, soldered connections, and glassy polymer substrate) are replaced with liquid-phase metal alloy and elastomer. This biomechanically compatible "soft-matter" PCB is rapidly produced (~3 h) using the same commercial UVLM system (Protolaser U3) used for conventional electronics prototyping. Since the circuit is composed entirely of soft and deformable material, fabrication does not depend on a limited selection of geometric patterns or the specialized microfabrication techniques required for thin-film metal circuits with deterministic architectures. In this respect, the proposed approach represents a relatively inexpensive, scalable, and user-accessible alternative that complements previous achievements in stretchable and thin-film electronics based on cleanroom lithography.

The intrinsic compliance of the soft-matter PCB is of particular importance in wearable bioelectronics and computing. For these applications, mechanical impedance mismatch can constrain natural body motion or cause irritation, discomfort, or tissue damage due to interfacial stress concentrations. Impedance matching is especially critical in optical or electrode-based bioelectronics applications, such as pulse oximetry, that depend on intimate contact with the skin for accurate physiological measurements. Incorporating soft materials, SSTs, and processing steps into a single UVLM-based fabrication method enables the rapid production of customizable wearables. Such systems could be user-/patient-specific and capable of physiological sensing for activity, fitness, and health monitoring.

While we have been able to report successful soft-matter PCB prototyping with UVLM, there remain plenty of opportunities for further exploration and improvement. In this manuscript, characterization was limited to a z-axis elastomer substrate. Additional studies are required to understand the influence of substrate material on EGaIn wetting and ablation. It is also worthwhile to examine nonsubtractive fabrication techniques that are compatible with conventional circuit printing. While UVLM processing is well-established for PCB prototyping, it has considerably higher materials waste than inkjet printing and other additive techniques. Lastly, the LED and pulseox demonstrations are intended to validate the fabrication method and compatibility of materials. Further efforts are needed to implement wireless, fully functional devices that have practical use for wearable computing and health monitoring.

■ ASSOCIATED CONTENT

Supporting Information

The Supporting Information is available free of charge on the ACS Publications website at DOI: 10.1021/acsami.7b05522.

Description of steps for fabrication of soft-matter PCBs, method for electrical characterization of circuits, details of the pulse oximetry circuit implementation, SEM images of coated/patterned and uncoated/unablated zPDMS, photographs of cross sections, configuration of the interdigitated capacitor, surface mount subjected to mechanical strain, and circuit diagram of LED array and pulse oximeter (PDF)

■ AUTHOR INFORMATION

Corresponding Author

*E-mail: cmajidi@andrew.cmu.edu. Phone: +1 (412) 268 2492.

DOI: 10.1021/acsami.7b05522
ACS Appl. Mater. Interfaces 2017, 9, 22055−22062

ORCID

Eric J. Markvicka: 0000-0002-5463-1567
Carmel Majidi: 0000-0002-6469-9645

Notes

The authors declare no competing financial interest.

■ ACKNOWLEDGMENTS

We acknowledge support from the NASA Early Career Faculty Award (NNX14AO49G; Research Collaborator: Dr. Bill Bluethmann), Office of Naval Research (Bioinspired Autonomous Systems; Dr. Tom McKenna; N00014-16-2301), and Disruptive Health Technology Institute. Circuit fabrication and characterization was performed on equipment supported through an ONR DURIP (Bioinspired Autonomous Systems; Dr. Tom McKenna; N00014140778).

■ REFERENCES

(1) Hammock, M. L.; Chortos, A.; Tee, B. C.-K.; Tok, J. B.-H.; Bao, Z. 25th Anniversary Article: The Evolution of Electronic Skin (E-Skin): A Brief History, Design Considerations, and Recent Progress. *Adv. Mater.* **2013**, *25*, 5997−6038.
(2) Gregory, R.; Kimbrell, W.; Kuhn, H. Conductive Textiles. *Synth. Met.* **1989**, *28*, 823−835.
(3) Ebneth, H. Metallized Textile Material. U.S. Patent 4,201,825, 1980.
(4) Neelakandan, R.; Madhusoothanan, M. Electrical Resistivity Studies on Polyaniline Coated Polyester Fabrics. *J. Eng. Fibers Fabr.* **2010**, *5*, 25−29.
(5) Klueh, U.; Wagner, V.; Kelly, S.; Johnson, A.; Bryers, J. Efficacy of Silver-Coated Fabric to Prevent Bacterial Colonization and Subsequent Device-Based Biofilm Formation. *J. Biomed. Mater. Res.* **2000**, *53*, 621−631.
(6) Kim, D.-H.; Kim, Y.-S.; Wu, J.; Liu, Z.; Song, J.; Kim, H.-S.; Huang, Y. Y.; Hwang, K.-C.; Rogers, J. A. Ultrathin Silicon Circuits with Strain-Isolation Layers and Mesh Layouts for High-Performance Electronics on Fabric, Vinyl, Leather, and Paper. *Adv. Mater.* **2009**, *21*, 3703−3707.
(7) Kim, D.; et al. Epidermal Electronics. *Science* **2011**, *333*, 838−843.
(8) Kim, D.-H.; Rogers, J. A. Stretchable Electronics: Materials Strategies and Devices. *Adv. Mater.* **2008**, *20*, 4887−4892.
(9) Rogers, J. A.; Someya, T.; Huang, Y. Materials and Mechanics for Stretchable Electronics. *Science* **2010**, *327*, 1603−1607.
(10) Sun, Y.; Rogers, J. A. Structural Forms of Single Crystal Semiconductor Nanoribbons for Highperformance Stretchable Electronics. *J. Mater. Chem.* **2007**, *17*, 832−840.
(11) Araki, T.; Nogi, M.; Suganuma, K.; Kogure, M.; Kirihara, O. Printable and Stretchable Conductive Wirings Comprising Silver Flakes and Elastomers. *IEEE Electron Device Lett.* **2011**, *32*, 1424−1426.
(12) Matsuhisa, N.; Kaltenbrunner, M.; Yokota, T.; Jinno, H.; Kuribara, K.; Sekitani, T.; Someya, T. Printable Elastic Conductors with a High Conductivity for Electronic Textile Applications. *Nat. Commun.* **2015**, *6*, 7461.
(13) Chun, K.-Y.; Oh, Y.; Rho, J.; Ahn, J.-H.; Kim, Y.-J.; Choi, H. R.; Baik, S. Highly Conductive, Printable and Stretchable Composite Films of Carbon Nanotubes and Silver. *Nat. Nanotechnol.* **2010**, *5*, 853−857.
(14) Larmagnac, A.; Eggenberger, S.; Janossy, H.; Vörös, J. Stretchable Electronics Based on Ag-PDMS Composites. *Sci. Rep.* **2015**, *4*, 7254.
(15) Niu, X.; Peng, S.; Liu, L.; Wen, W.; Sheng, P. Characterizing and Patterning of PDMS-Based Conducting Composites. *Adv. Mater.* **2007**, *19*, 2682−2686.
(16) Cao, Q.; Kim, H.; Pimparkar, N.; Kulkarni, J.; Wang, C.; Shim, M.; Roy, K.; Alam, M.; Rogers, J. Medium-Scale Carbon Nanotube Thin-Film Integrated Circuits on Flexible Plastic Substrates. *Nature* **2008**, *454*, 495−502.
(17) Lipomi, D.; Vosgueritchian, M.; Tee, B.; Hellstrom, S.; Lee, J.; Fox, C.; Bao, Z. Skin-Like Pressure and Strain Sensors Based on Transparent Elastic Films of Carbon Nanotubes. *Nat. Nanotechnol.* **2011**, *6*, 788−792.
(18) Xia, Y.; Ouyang, J. PEDOT:PSS Films with Significantly Enhanced Conductivities Induced by Preferential Solvation with Cosolvents and Their Application in Polymer Photovoltaic Cells. *J. Mater. Chem.* **2011**, *21*, 4927−4936.
(19) Stoyanov, H.; Kollosche, M.; Risse, S.; Waché, R.; Kofod, G. Soft Conductive Elastomer Materials for Stretchable Electronics and Voltage Controlled Artificial Muscles. *Adv. Mater.* **2013**, *25*, 578−583.
(20) Liu, C.-X.; Choi, J.-W. Embedding Conductive Patterns of Elastomer Nanocomposite with the Assist of Laser Ablation. *Microsyst. Technol.* **2012**, *18*, 365−371.
(21) Muth, J. T.; Vogt, D. M.; Truby, R. L.; Mengüç, Y.; Kolesky, D. B.; Wood, R. J.; Lewis, J. A. Embedded 3D Printing of Strain Sensors within Highly Stretchable Elastomers. *Adv. Mater.* **2014**, *26*, 6307−6312.
(22) Weigel, M.; Lu, T.; Bailly, G.; Oulasvirta, A.; Majidi, C.; Steimle, J. Iskin: Flexible, Stretchable and Visually Customizable On-Body Touch Sensors for Mobile Computing. *Proc. 33rd Annu. ACM Conf. Hum. Factors Comput. Sys.* **2015**, 2991−3000.
(23) Cheng, S.; Wu, Z. Microfluidic Electronics. *Lab Chip* **2012**, *12*, 2782−2791.
(24) Dickey, M. D. Emerging Applications of Liquid Metals Featuring Surface Oxides. *ACS Appl. Mater. Interfaces* **2014**, *6*, 18369−18379.
(25) Dickey, M. D.; Chiechi, R. C.; Larsen, R. J.; Weiss, E. A.; Weitz, D. A.; Whitesides, G. M. Eutectic gallium-indium (EGaIn): a Liquid Metal Alloy for the Formation of Stable Structures in Microchannels at Room Temperature. *Adv. Funct. Mater.* **2008**, *18*, 1097−1104.
(26) Joshipura, I. D.; Ayers, H. R.; Majidi, C.; Dickey, M. D. Methods to Pattern Liquid Metals. *J. Mater. Chem. C* **2015**, *3*, 3834−3841.
(27) Chiechi, R. C.; Weiss, E. A.; Dickey, M. D.; Whitesides, G. M. Eutectic Gallium-Indium (EGaIn): A Moldable Liquid Metal for Electrical Characterization of Self-Assembled Monolayers. *Angew. Chem.* **2008**, *120*, 148−150.
(28) Doudrick, K.; Liu, S.; Mutunga, E. M.; Klein, K. L.; Damle, V.; Varanasi, K. K.; Rykaczewski, K. Different Shades of Oxide: From Nanoscale Wetting Mechanisms to Contact Printing of Gallium-Based Liquid Metals. *Langmuir* **2014**, *30*, 6867−6877.
(29) Liu, T.; Sen, P.; Kim, C. Characterization of Nontoxic Liquid-Metal Alloy Galinstan for Applications in Microdevices. *J. Microelectromech. Syst.* **2012**, *21*, 443−450.
(30) Khondoker, M.; Sameoto, D. Fabrication Methods and Applications of Microstructured Gallium Based Liquid Metal Alloys. *Smart Mater. Struct.* **2016**, *25*, 093001.
(31) Jeong, S. H.; Hagman, A.; Hjort, K.; Jobs, M.; Sundqvist, J.; Wu, Z. Liquid Alloy Printing of Microfluidic Stretchable Electronics. *Lab Chip* **2012**, *12*, 4657−4664.
(32) Jeong, S. H.; Hjort, K.; Wu, Z. Tape Transfer Atomization Patterning of Liquid Alloys for Microfluidic Stretchable Wireless Power Transfer. *Sci. Rep.* **2015**, *5*, 8419.
(33) Kramer, R. K.; Majidi, C.; Wood, R. J. Masked Deposition of Gallium-Indium Alloys for Liquid-Embedded Elastomer Conductors. *Adv. Funct. Mater.* **2013**, *23*, 5292−5296.
(34) Li, G.; Wu, X.; Lee, D.-W. Selectively Plated Stretchable Liquid Metal Wires for Transparent Electronics. *Sens. Actuators, B* **2015**, *221*, 1114−1119.
(35) Khan, M. R.; Bell, J.; Dickey, M. D. Localized Instabilities of Liquid Metal Films via In-Plane Recapillarity. *Adv. Mater. Interfaces* **2016**, *3*, 1600546.
(36) Tabatabai, A.; Fassler, A.; Usiak, C.; Majidi, C. Liquid-Phase Gallium-Indium Alloy Electronics with Microcontact Printing. *Langmuir* **2013**, *29*, 6194−6200.

DOI: 10.1021/acsami.7b05522
ACS Appl. Mater. Interfaces 2017, 9, 22055−22062

(37) Gozen, B. A.; Tabatabai, A.; Ozdoganlar, O. B.; Majidi, C. High-Density Soft-Matter Electronics with Micron-Scale Line Width. *Adv. Mater.* **2014**, *26*, 5211−5216.
(38) Wang, Q.; Yu, Y.; Yang, J.; Liu, J. Fast Fabrication of Flexible Functional Circuits Based on Liquid Metal Dual-Trans Printing. *Adv. Mater.* **2015**, *27*, 7109−7116.
(39) Li, G.; Wu, X.; Lee, D.-W. A Galinstan-Based Inkjet Printing System for Highly Stretchable Electronics with Self-Healing Capability. *Lab Chip* **2016**, *16*, 1366−1373.
(40) Ladd, C.; So, J.-H.; Muth, J.; Dickey, M. D. 3D Printing of Free Standing Liquid Metal Microstructures. *Adv. Mater.* **2013**, *25*, 5081−5085.
(41) Boley, J. W.; White, E. L.; Chiu, G. T.-C.; Kramer, R. K. Direct Writing of Gallium-Indium Alloy for Stretchable Electronics. *Adv. Funct. Mater.* **2014**, *24*, 3501−3507.
(42) Gannarapu, A.; Gozen, B. A. Freeze-Printing of Liquid Metal Alloys for Manufacturing of 3D, Conductive, and Flexible Networks. *Adv. Mater. Technol.* **2016**, *1*, 1600047.
(43) Vogt, D. M.; Wood, R. J. Wrist angle measurements using soft sensors. *2014 IEEE Sensors* **2014**, 1631−1634.
(44) Menguc, Y.; Park, Y.-L.; Pei, H.; Vogt, D.; Aubin, P. M.; Winchell, E.; Fluke, L.; Stirling, L.; Wood, R. J.; Walsh, C. J. Wearable Soft Sensing Suit for Human Gait Measurement. *nt. J. Robot. Res.* **2014**, *33*, 1748−1764.
(45) Overvelde, J. T. B.; Mengüç, Y.; Polygerinos, P.; Wang, Y.; Wang, Z.; Walsh, C. J.; Wood, R. J.; Bertoldi, K. Mechanical and Electrical Numerical Analysis of Soft Liquid-Embedded Deformation Sensors Analysis. *Extreme Mechanics Letters* **2014**, *1*, 42−46.
(46) Kim, S.; Lee, J.; Choi, B. Stretching and Twisting Sensing with Liquid-Metal Strain Gauges Printed on Silicone Elastomers. *IEEE Sens. J.* **2015**, *15*, 6077−6078.
(47) Jung, T.; Yang, S. Highly Stable Liquid Metal-Based Pressure Sensor Integrated with a Microfluidic Channel. *Sensors* **2015**, *15*, 11823−11835.
(48) Choi, J.; Kim, S.; Lee, J.; Choi, B. Improved Capacitive Pressure Sensors based on Liquid Alloy and Silicone Slastomer. *IEEE Sens. J.* **2015**, *15*, 4180−4181.
(49) Michaud, H. O.; Teixidor, J.; Lacour, S. P. Soft Flexion Sensors Integrating Strechable Metal Conductors on a Silicone Substrate for Smart Glove Applications. *2015 28th IEEE Inter. Conf. MEMS* **2015**, 760−763.
(50) Matsuzaki, R.; Tabayashi, K. Highly Stretchable, Global, and Distributed Local Strain Sensing Line using GaInSn Electrodes for Wearable Electronics. *Adv. Funct. Mater.* **2015**, *25*, 3806−3813.
(51) Codd, P. J.; Veaceslav, A.; Gosline, A. H.; Dupont, P. E. Novel Pressure-Sensing Skin for Detecting Impending Tissue Damage During Neuroendoscopy: Laboratory Investigation. *J. Neurosurg.* **2014**, *13*, 114−121.
(52) Liu, P.; Yang, S.; Jain, A.; Wang, Q.; Jiang, H.; Song, J.; Koschny, T.; Soukoulis, C. M.; Dong, L. Tunable Meta-Atom using Liquid Metal Embedded in Stretchable Polymer. *J. Appl. Phys.* **2015**, *118*, 014504.
(53) Ling, K.; Kim, H. K.; Yoo, M.; Lim, S. Frequency-Switchable Metamaterial Absorber Injecting Eutectic Gallium-Indium (EGaIn) Liquid Metal Alloy. *Sensors* **2015**, *15*, 28154−28165.
(54) Hayes, G. J.; Liu, Y.; Genzer, J.; Lazzi, G.; Dickey, M. D. Self-Folding Origami Microstrip Antennas. *IEEE Trans. Antennas Propag.* **2014**, *62*, 5416−5419.
(55) Gough, R. C.; Morishita, A. M.; Dang, J. H.; Hu, W.; Shiroma, W. A.; Ohta, A. T. Continuous Electrowetting of Non-Toxic Liquid Metal for RF Applications. *IEEE Access* **2014**, *2*, 874−882.
(56) Koo, C.; LeBlanc, B. E.; Kelley, M.; Fitzgerald, H. E.; Huff, G. H.; Han, A. Manipulating Liquid Metal Droplets in Microfluidic Channels With Minimized Skin Residues Toward Tunable RF Applications. *J. Microelectromech. Syst.* **2015**, *24*, 1069−1076.
(57) Wu, Z.; Hjort, K.; Jeong, S. H. Microfluidic Stretchable Radio-Frequency Devices. *Proc. IEEE* **2015**, *103*, 1211−1225.
(58) Saghati, A. P.; Batra, J. S.; Kameoka, J.; Entesari, K. Miniature and Reconfigurable CPW Folded Slot Antennas Employing Liquid-Metal Capacitive Loading. *IEEE Trans. Antennas Propag.* **2015**, *63*, 3798−3807.
(59) Wang, M.; Trlica, C.; Khan, M. R.; Dickey, M. D.; Adams, J. J. A Reconfigurable Liquid Metal Antenna Driven by Electrochemically Controlled Capillarity. *J. Appl. Phys.* **2015**, *117*, 194901.
(60) Kim, D.; Yoo, J. H.; Lee, J.-B. Liquid Metal-Based Reconfigurable and Stretchable Photolithography. *J. Micromech. Microeng.* **2016**, *26*, 045004.
(61) Memon, M. U.; Ling, K.; Seo, Y.; Lim, S. Frequency-Switchable Half-Mode Substrate-Integrated Waveguide Antenna Injecting Eutectic Gallium Indium (EGaIn) Liquid Metal Alloy. *J. Electromagnetic Wave* **2015**, *29*, 2207−2215.
(62) Lu, T.; Wissman, J.; Ruthika; Majidi, C. Soft Anisotropic Conductors as Electric Vias for Ga-Based Liquid Metal Circuits. *ACS Appl. Mater. Interfaces* **2015**, *7*, 26923−26929.
(63) Lu, T.; Finkenauer, L.; Wissman, J.; Majidi, C. Rapid Prototyping for Soft-Matter Electronics. *Adv. Funct. Mater.* **2014**, *24*, 3351−3356.
(64) Mendelson, Y. Pulse Oximetry: Theory and Applications for Noninvasive Monitoring. *Clin. Chem.* **1992**, *38*, 1601−1607.
(65) Gao, L.; Zhang, Y.; Malyarchuk, V.; Jia, L.; Jang, K.-I.; Webb, R. C.; Fu, H.; Shi, Y.; Zhou, G.; Shi, L.; et al. Epidermal photonic devices for quantitative imaging of temperature and thermal transport characteristics of the skin. *Nat. Commun.* **2014**, *5*, 4938.
(66) Yokota, T.; Zalar, P.; Kaltenbrunner, M.; Jinno, H.; Matsuhisa, N.; Kitanosako, H.; Tachibana, Y.; Yukita, W.; Koizumi, M.; Someya, T. Ultraflexible Organic Photonic Skin. *Sci. Adv.* **2016**, *2*, e1501856.
(67) Gevorgian, S. S.; Martinsson, T.; Linner, P. L.; Kollberg, E. L. CAD Models for Multilayered Substrate Interdigital Capacitors. *IEEE Trans. Microwave Theory Tech.* **1996**, *44*, 896−904.
(68) McKenzie, D.; McPhedran, R. ExactModelling of Cubic Lattice Permittivity and Conductivity. *Nature* **1977**, *265*, 128−129.
(69) Bartlett, M. D.; Markvicka, E. J.; Majidi, C. Rapid Fabrication of Soft, Multilayered Electronics for Wearable Biomonitoring. *Adv. Funct. Mater.* **2016**, *26*, 8496−8504.
(70) Murray, W. B.; Foster, P. A. The Peripheral Pulse Wave: Information Overlooked. *J. Clin. Monitor.* **1996**, *12*, 365−377.

DOI: 10.1021/acsami.7b05522
ACS Appl. Mater. Interfaces 2017, 9, 22055−22062